



ORIGINAL PAPER

A NEW METHOD OF DETERMINING THE PERIOD-DEPENDENT LAYER HEIGHT FOR IONOSPHERIC MODELLING

Zeyin HU

China Railway Design Corporation, Tianjin 300251, China

Corresponding author's e-mail: hu_zeyin@126.com**ARTICLE INFO****Article history:**

Received 31 March 2025

Accepted 10 June 2025

Available online 30 June 2025

Keywords:

Period-dependent layer of ionosphere hypothesis

Ionospheric effective height
Ionospheric modeling**ABSTRACT**

Due to the time-varying characteristics of the peak height of ionospheric electron density, this article determines the period-dependent layer height for ionospheric modeling based on the minimum difference between the vertical total electron contents (VTEC) provided by final global ionospheric map (GIM) product and the measured slant total electron contents (STEC). Based on the period-dependent layer height model for ionospheric, a polynomial model is used to model the ionosphere in the study area. Compared to the fixed period-dependent layer height model, the period-dependent layer height model for ionospheric has an accuracy improvement of 14 % in satellite differential code bias (SDCB) estimation, and the fitting accuracy has been improved by 16 % at the verification station. The experimental results demonstrate that the period-dependent layer height model can effectively explain the vertical distribution of the ionosphere.

1. INTRODUCTION

The ionosphere is one of the most dynamic regions in Earth's atmospheric space, exerting significant physical and chemical effects on radio signals, influencing their propagation direction and power (Schafer, 1999). Therefore, ionospheric modeling based on Global Navigation Satellite System (GNSS) signals has become one of the most effective approaches (Li, 2012; Wang, 2017; Xu et al., 2021; Xu et al., 2020). While dual-frequency GNSS users mitigate ionospheric delays through observable combinations, single-frequency users rely on ionospheric correction models (Xu, 2019; Yuan, 2002; Yuan et al., 2017; Xu et al., 2022). To simplify ionospheric distribution, it is commonly assumed that ionospheric electrons are concentrated on an infinitesimally period-dependent layer shell, known as the single-layer model (SLM) (Li et al., 2019). Determining the optimal height of this period-dependent layer shell remains a critical research focus.

Currently, most ionospheric products released by the International GNSS Service (IGS) Ionosphere Associate Analysis Centers (IAAC) adopt SLM with fixed period-dependent layer heights between 350–450 km, derived from global averages of ionospheric electron density peak heights (Lanyi and Roth, 1988; Brunini et al., 2011). However, SLM exhibits two limitations: (1) it neglects temporal variations in electron density peak heights, and (2) the assumption of symmetric electron distribution around ionospheric penetration points (IPPs) contradicts the anisotropic

nature of the ionosphere (Mannucci et al., 1999). Komjathy et al. (2005) reported projection errors up to 10 m during geomagnetic storms. Studies indicate that varying the period-dependent layer height from 250 km to 800 km introduces up to 8 TECu errors in ionospheric models (Wang et al., 2016). Prior studies on regional period-dependent layer height determination include Brich et al. (2002) optimized IEH to 750 km for the UK using zenith and slant path observations. Methods minimizing discrepancies between dual-path measurements at shared IPPs (Nava et al., 2007). Zhao and Zhou's DCB-based optimization (Zhao and Zhou, 2018). Li et al.'s GIM-referenced approach (450–550 km optimal for China) (Li et al., 2018). Xu et al.'s neural network-based variable-height model (Xu et al., 2023). While neural networks achieve high accuracy, their computational demands are prohibitive. This study proposes a time-segmented period-dependent layer height determination method using IGS final GIM VTEC and measured STEC to minimize projection errors, validated through experiments.

2. DETERMINATION OF IONOSPHERIC HEIGHT MODEL

To obtain high-precision original ionospheric observation information, this study employs the single-frequency PPP technique to derive STEC true values from GPS observations, as follows:

$$\begin{cases} P_{1,r}^s - \rho_r^s \Big|_0 + \overline{c dt^s} = \Delta e \Delta \mathbf{r} + c dt_{1,r} + T_{1,r}^s + I_{1,r}^s + \Omega_p \\ L_{1,r}^s - \rho_r^s \Big|_0 + \overline{c dt^s} = \Delta e \Delta \mathbf{r} + c dt_{1,r} + T_{1,r}^s - I_{1,r}^s + N_{1,r}^s + \Omega_L \end{cases} \quad (1)$$

where $P_{1,r}^s, L_{1,r}^s$ represent the pseudorange and carrier phase observations on the L1 frequency (unit: m and cycles, respectively), $\rho_r^s \Big|_0$ denotes the approximate geometric distance calculated from precise ephemeris and initial station coordinates (unit: m), $\overline{c dt^s}$ is the precise satellite clock offset from official products (unit: s), Δe indicates the line-of-sight vector from receiver to satellite, $\Delta \mathbf{r}$ represents the station coordinate increment to be estimated (unit: m), $c dt_{1,r}$ is receiver clock offset parameter to be estimated (unit: s), $T_{1,r}^s$ stands for the tropospheric delay parameter

(unit: m), $I_{1,r}^s$ is the ionospheric delay parameter on L1 (unit: m), $N_{1,r}^s$ corresponds to the float ambiguity term (unit: m), Ω_p encompass other pseudorange errors: antenna phase center correction, tidal loading, solid Earth tide, etc.

Since the satellite clock datum aligns with L1 and L2 observations, hardware delays (e.g., Differential Code Bias, DCB) are absorbed, as shown in Equation (2):

$$\overline{c dt^s} = c dt^s - \left(\frac{\beta_{2,p}}{\beta_{2,p} - \beta_{1,p}} d_{1,p}^s - \frac{\beta_{1,p}}{\beta_{2,p} - \beta_{1,p}} d_{2,p}^s \right) \quad (2)$$

where $\beta_{m,p}$ is the frequency of the m-th signal (unit: Hz), defined as $\beta_{m,p} = \frac{f_{1,m}^2}{f_1^2}$, $d_{1,p}^s, d_{2,p}^s$ denotes the satellite pseudorange hardware delay between L1 and L2 (unit: m).

Thus, in Equation (1):

$$\begin{cases} dt_{1,r} = dt_{1,r} + \left(\frac{\beta_{2,p}}{\beta_{2,p} - \beta_{1,p}} d_{1,r,p} - \frac{\beta_{1,p}}{\beta_{2,p} - \beta_{1,p}} d_{2,r,p} \right) \\ I_{1,r}^s = \beta_{1,p}^s \left(I_{r,1}^{s,g} - \frac{1}{\beta_{2,p} - \beta_{1,p}} (DCB_{1,2,r} + DCB_{1,2}^s) \right) \\ N_{1,r}^s = \frac{c}{f_1} \overline{N_{1,r}^s} - (d_{1,r,p} + d_{1,p}^s) \end{cases} \quad (3)$$

where $I_{r,1}^{s,g}$ is the pure ionospheric delay on the L1 frequency, $DCB_{1,2,r} = d_{r,1,p} - d_{r,2,p}$ denotes the Satellite Differential Code Bias (SDCB) between L1 and other signals (unit: m), $DCB_{1,2}^s = d_{1,p}^s - d_{2,p}^s$ represents the Satellite Differential Code Bias (SDCB) (unit: m), $\overline{N_{1,r}^s}$ is the ambiguity term incorporating phase fractional biases, c denotes the speed of light in vacuum (299792458m/s), f_1 is the frequency of the L1.

Since the ionospheric parameters, ambiguity terms and clock offsets in Equation (1) cannot be

uniquely estimated, we apply constraints to the clock offset at the first epoch and reparameterize it as:

$$\begin{cases} P_{1,r}^s(k) - \rho_r^s \Big|_0(k) + \overline{c dt^s(k)} \\ = \Delta e \Delta \mathbf{r}(k) + c \Delta dt_{1,r}(k) + T_{1,r}^s + I_{1,r}^s(k) + \Omega_p \\ L_{1,r}^s(k) - \rho_r^s \Big|_0(k) + \overline{c dt^s(k)} \\ = \Delta e \Delta \mathbf{r}(k) + c \Delta dt_{1,r}(k) + T_{1,r}^s - I_{1,r}^s(k) + N_{1,r}^s(k) + \Omega_L \end{cases} \quad (4)$$

in the above formula,

$$\begin{cases} \Delta dt_{1,r}(k) = dt_{1,r}(k) - dt_{1,r}(1) + \overline{dt_{1,r}} \\ I_{1,r}^s(k) = I_{1,r}^s(k) + c \left(dt_{1,r}(1) - \overline{dt_{1,r}} \right) \\ N_{1,r}^s(k) = N_{1,r}^s(k) + 2c \left(dt_{1,r}(1) - \overline{dt_{1,r}} \right) \end{cases} \quad (5)$$

where $\overline{dt_{1,r}}$ represents the constrained clock offset at the first epoch. During PPP processing, official DCB products are applied to correct DCB effects, yielding refined ionospheric delays for period-dependent layer height modeling.

The final Global Ionospheric Map (GIM) products achieve the highest ionospheric fitting accuracy, with errors ranging from 2 to 8 TECu (Li, 2012). In this study, the VTEC values derived from GIM are regarded as true values. The following steps are implemented to determine the optimal period-dependent layer height:

1. Candidate Period-Dependent Layer Heights: 100 to 2,000 km with 50 km intervals (total 39 candidate heights).
2. Temporal Segmentation: The day is divided into 6 epochs (00:00–04:00, 04:00–08:00, ..., 20:00–24:00 UTC).

$$E(i) = RMS \left(VTEC - \frac{STEC}{MF(h)} \right)$$

$$i \in (1, 6) \quad \{h|h = 100 + 50n, n = 0, 1, 2, \dots, 38\}$$

3. RMSE Calculation: At each candidate height h , the Root Mean Square Error (RMSE) between the observed VTEC and GIM-based VTEC is computed as:

$$RMSE(h) = \sqrt{\frac{1}{N} \sum_{i=1}^N \left(VTEC_{GIM}^i - \frac{SETC_{obs}^i}{MF(h)} \right)^2}$$

where $VTEC_{GIM}^i$ is VTEC true value interpolated from GIM at the i-th Ionospheric Pierce Point (IPP), $SETC_{obs}^i$ denotes the observed STEC at the i-th IPP (unit: TECu). $MF(h)$ is mapping function at height h , defined as

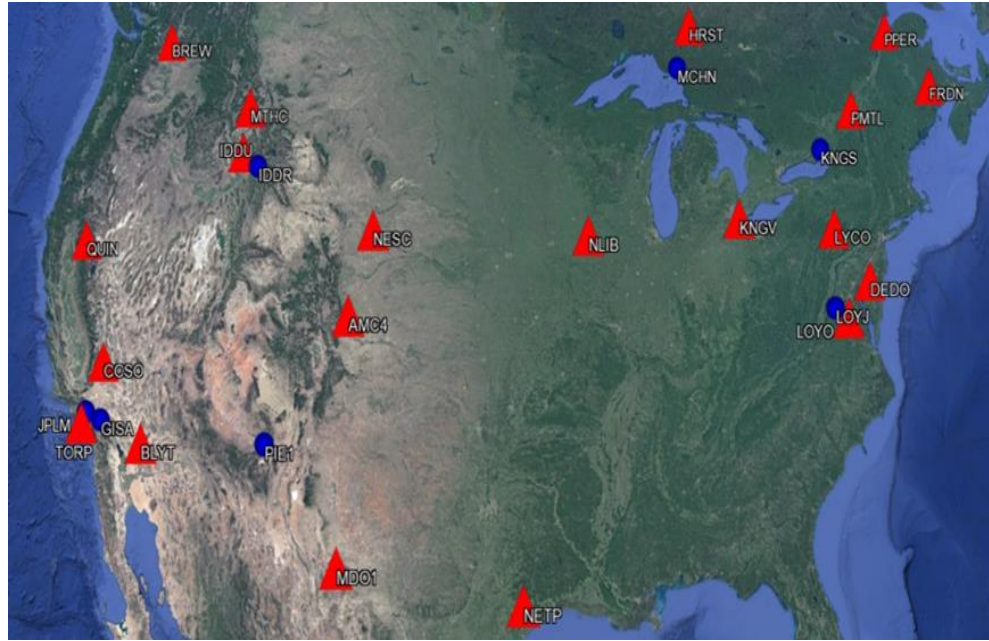


Fig. 1 Station distribution map (red triangles indicate modeling stations; blue circles denote validation stations).

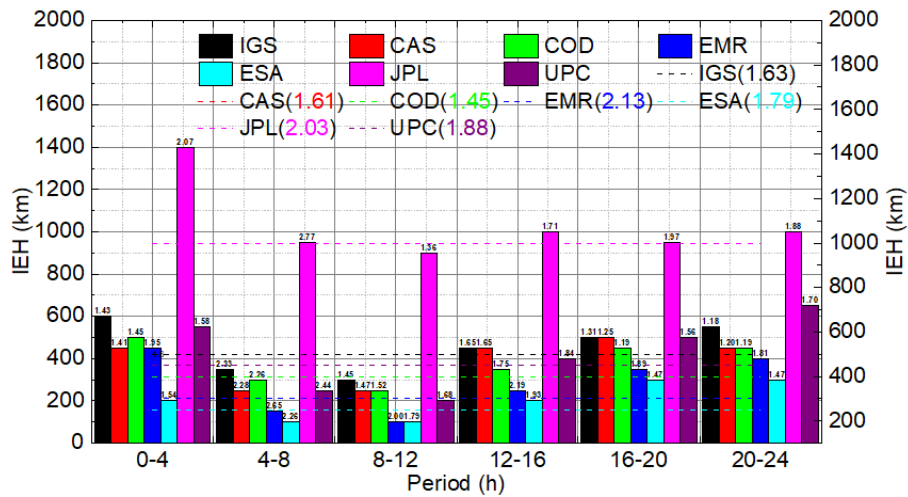


Fig. 2 Histogram of epoch-wise period-dependent layer height distribution.

$$MF(h) = \frac{1}{\cos \alpha_i} = \frac{1}{\sqrt{1 - \left(\frac{R_E}{R_E + h} \cos(\theta)\right)^2}}$$

where $R_E = 6,378$ km (Earth’s radius) and θ is the satellite elevation angle.

4. Optimal Height Selection: The height corresponding to the minimum RMSE within each epoch is selected as the optimal period-dependent layer height.

3. MODEL CONSTRUCTION AND ACCURACY VALIDATION

This study utilizes 27 stations from the U.S. CORS network on day of year (DOY) 102 in 2021, including 20 modeling stations and 7 validation

stations. The spatial distribution of these stations is shown in Figure 1. The data processing strategy for UUPPP is configured as follows: The satellite elevation cutoff angle is set to 10°, the data sampling interval is 30 seconds, and ionospheric parameters are estimated as white-noise processes along with station coordinates. Additionally, float ambiguity parameters and tropospheric delays are output during the processing.

Figure 2 displays the epoch-wise optimal period-dependent layer heights derived using VTEC from seven analysis centers as ground-truth references. The seven analysis centers include the International GNSS Service (IGS), the Center for Orbit Determination in Europe (CODE), the European Space Operations

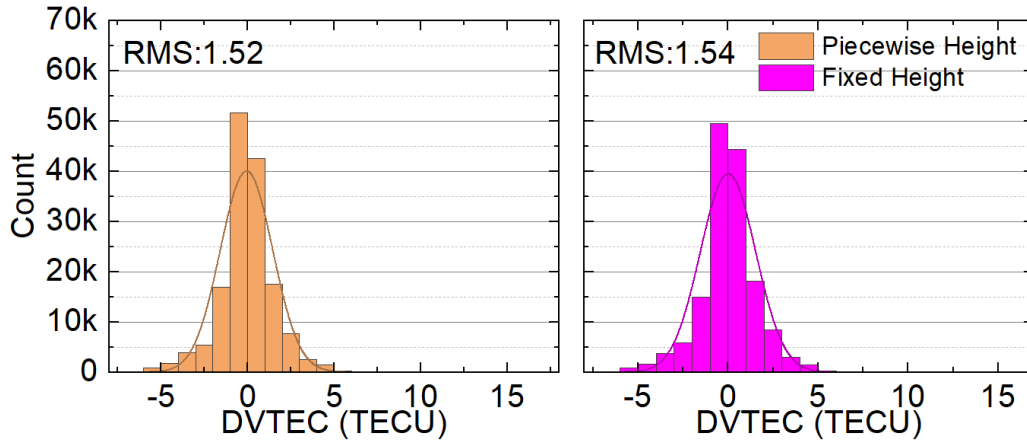


Fig. 3 Frequency distribution histogram of DVTEC from epoch-wise and fixed-layer height models at validation stations.

Center of European Space Agency (ESOC), the Jet Propulsion Laboratory (JPL), the Technical University of Catalonia/gAGE (UPC), the Natural Resource Canada (EMR), and the Chinese Academy of Sciences (CAS). In the histogram, the bar heights represent the root mean square error (RMSE) of period-dependent layer heights, dashed lines indicate the optimal period-dependent layer heights calculated using full-day data, and numerical values in the legend correspond to the RMSE of fixed-layer heights. Key observations from the figure are as follows: (1) Inter-GIM height variability: Significant discrepancies exist between period-dependent layer heights derived from different GIM products. For instance, within the 0–4 UT interval, the height difference between JPL and ESA results reaches up to 1,200 km. (2) Temporal variations within a single GIM: The optimal period-dependent layer height for a single GIM varies across epochs, with a maximum difference of 450 km observed in UPC results between 20–24 UT and 8–12 UT. This highlights the necessity of epoch-wise height determination. (3) Full-day inter-GIM divergence: The maximum height difference between GIMs over the entire day is 750 km. (4) Intra-GIM RMSE stability: The minimum RMSE differences for a single GIM across epochs remain within 1 TECu. (5) Minimum RMSE Consistency and GIM Performance: The differences in minimum RMSE among all GIMs remain within 1 TECu. Notably, the JPL GIM exhibits the largest minimum RMSE (i.e., the poorest performance) and consequently yields the highest optimal period-dependent layer height. This arises because JPL generates its GIM by directly interpolating observed IPP data, which introduces significant errors in regions with sparse data coverage. In contrast, the IGS final GIM combines products from other analysis centers through weighted averaging, achieving the highest accuracy. Therefore, this study adopts the IGS GIM as the ground truth for IPP VTEC extraction.

Figure 3 shows the frequency distribution of Differential VTEC (DVTEC) values calculated at 7 validation stations using two models: (a) The fixed-layer height model (optimal height derived from full-day GIM data). (b) The epoch-wise period-dependent layer height model (optimal height determined for each epoch).

Key observations from Figure 3: (a) Compared to the fixed-layer model, the DVTEC values from the epoch-wise model are more clustered around smaller magnitudes and approximately follow a normal distribution. (b) The epoch-wise model achieves a DVTEC RMSE of 1.52 TECu, outperforming the fixed-layer model (1.54 TECu).

These results demonstrate that the epoch-wise period-dependent layer height model better captures the vertical ionospheric structure compared to the fixed-height approach.

To further validate the application efficacy of the epoch-wise period-dependent layer height model in ionospheric modeling, this study employs observational data from 20 stations. The ionospheric observables are obtained through the Carrier-Smoothed Pseudorange (CSP) algorithm, and the ionospheric distribution over the U.S. region is modeled using a 4th-order polynomial, as expressed in Equation (7).

$$\begin{cases} VTEC(\varphi, \lambda, t) \\ = \sum_{n=0}^4 \sum_{m=0}^4 [E_{nm} (\varphi - \varphi_0)^n (\lambda - \lambda_0 + t - t_0)^m] \\ STEC(\varphi, \lambda, t) \\ = VTEC(\varphi, \lambda, t) * MF(h) \end{cases} \quad (7)$$

In the equation, $VTEC(\varphi, \lambda, t)$ and $STEC(\varphi, \lambda, t)$ represent the vertical (zenith) and slant ionospheric electron content at the Ionospheric Pierce Point (IPP), respectively (units: TECu). φ and φ_0 denote the geographic latitude of the IPP and the study

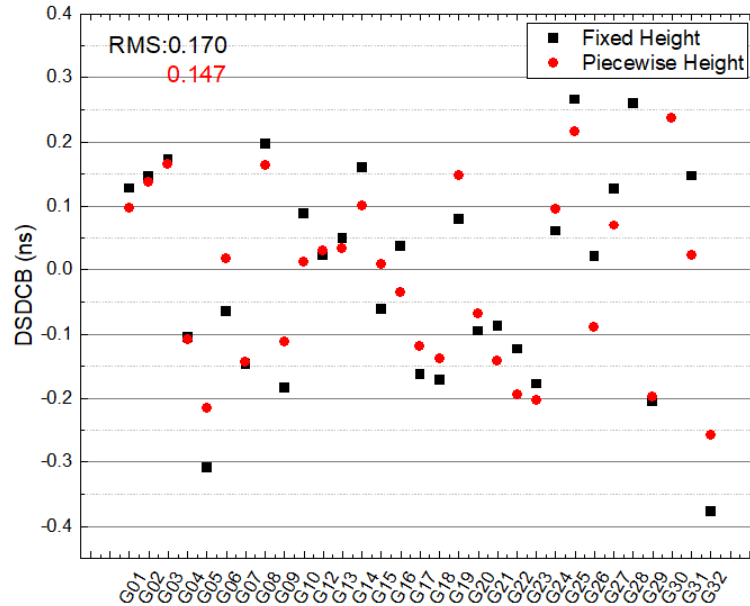


Fig. 4 Discrepancy series between SDCB estimated by fixed-layer and epoch-wise height models against CAS SDCB references.

region’s central latitude (unit: degrees). λ and λ_0 indicate the geographic longitude of the IPP and the study region’s central longitude (unit: degrees). t is the observation time expressed in Modified Julian Date (MJD), and t_0 represents the solar zenith angle at the IPP (unit: radians). E_{nm} corresponds to the polynomial coefficients to be estimated through least-squares fitting.

Figure 4 presents the discrepancy sequences between satellite differential code biases (SDCB) estimated by fixed-layer and epoch-wise height models against CAS-published SDCB references. Results demonstrate that the epoch-wise model achieves smaller deviations, with a DSDCB RMS of 0.147 ns compared to 0.170 ns for the fixed model, yielding a 14 % precision improvement. Figure 5 displays residual boxplots of polynomial models constructed under both height frameworks. The boxplots reveal that the polynomial model residuals from the epoch-wise height model are distributed within a narrower range with fewer outliers. Specifically, the fixed-layer model exhibits a $1.5 \times$ interquartile range (IQR) spanning from -2.39 to 2.40 TECu, while the epoch-wise model achieves a tighter range of -2.19 to 2.21 TECu. This quantitatively demonstrates that the epoch-wise height-based polynomial model better captures the time-varying characteristics of the ionosphere over the United States. To further validate model efficacy, Figure 6 illustrates the frequency distributions of fitting residuals at 7 validation stations, where SDCB and receiver differential code biases (RDCB) were derived via post-processed ionospheric modeling. The epoch-wise polynomial model achieves a residual standard deviation of 0.98 TECu, outperforming the fixed model (1.16 TECu) by 16 %. Collectively, these

results validate that the epoch-wise period-dependent layer height model provides enhanced vertical ionospheric representation, delivering improved internal and external consistency in ionospheric modeling accuracy.

4. CONCLUSIONS

To address the inadequacy of the traditional period-dependent layer height assumption in representing vertical ionospheric structures, this study proposes an epoch-wise period-dependent layer height determination method based on the ionosphere’s diurnal variations. By utilizing IGS final GIM VTEC as ground truth and minimizing RMSE between PPP-derived STEC and reference values, optimal period-dependent layer heights were determined for distinct time epochs. Experimental validation using 27 U.S. CORS stations (DOY 102, 2021) confirms the efficacy of this approach.

First, discrepancies in period-dependent layer heights derived from seven GIM products (IGS, CODE, ESOC, JPL, UPC, EMR, CAS) were analyzed. Results reveal significant inter-GIM differences (up to 1,200 km) and intra-GIM temporal variations (≤ 450 km), justifying epoch-wise modeling. Despite these variations, RMSE differences among GIMs remained within 2 TECu. Notably, JPL’s height estimates diverged markedly due to its direct interpolation strategy in data-sparse regions. The IGS GIM, synthesized through weighted integration of multi-center products, demonstrated superior accuracy and was adopted as the VTEC reference. At modeling stations, the epoch-wise model achieved smaller VTEC-GIM deviations.

Second, ionospheric variations over the U.S. were modeled using a 4th-order polynomial under

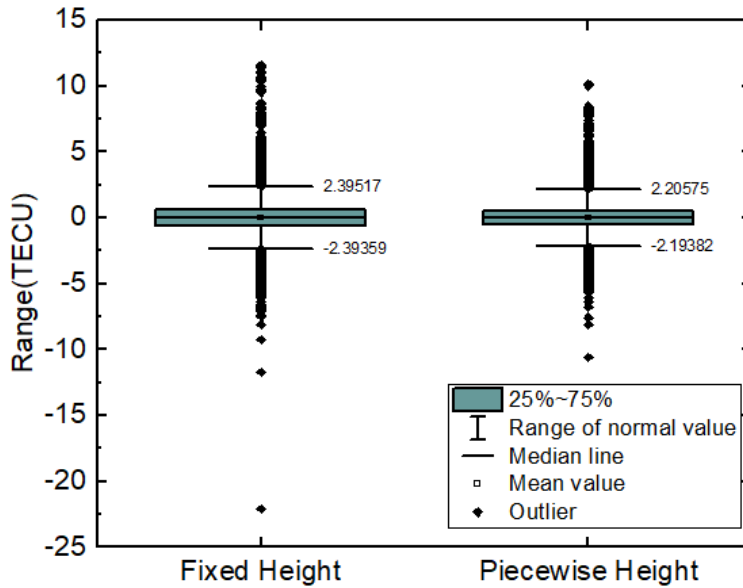


Fig. 5 Boxplots of ionospheric modeling residuals for fixed-layer and epoch-wise period-dependent layer height models.

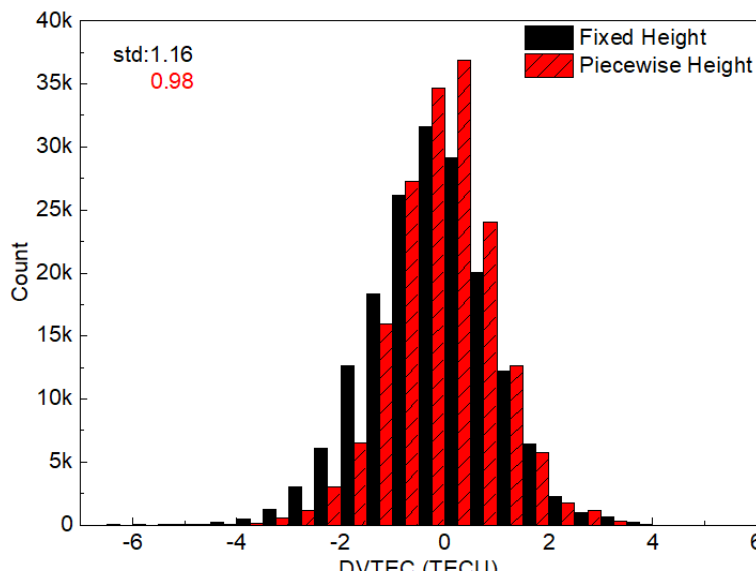


Fig. 6 Frequency distribution histogram of ionospheric model fitting residuals for fixed-layer and period-dependent layer height model.

both fixed-layer and epoch-wise frameworks. The epoch-wise model improved SDCB estimation accuracy by 14 % (0.147 ns vs. 0.170 ns RMSE) and reduced validation residuals by 16 % (0.98 TECu vs. 1.16 TECu standard deviation). These enhancements stem from the model’s ability to better characterize time-dependent ionospheric behaviors, as evidenced by tighter residual distributions (IQR: -2.19–2.21 TECu) compared to fixed-layer results (IQR: -2.39–2.40 TECu).

Collectively, the period-dependent layer height model for ionospheric significantly advances ionospheric representation, improving both internal

consistency (model fitting) and external accuracy (validation performance). Future work will extend this framework to regional-global hybrid modeling and multi-constellation integration.

ACKNOWLEDGEMENT

This article was sponsored by Research Fund of China Railway Design Corporation (2023A0240103 - Theoretical and Methodological Research on High-Precision Measurement and Control Technology for Subsea Ultra-Long Tunnel in the Bohai Strait Cross-Sea Passage).

REFERENCES

- Birch, M.J., Hargreaves, J.K. and Bailey, G.J.: 2002, On the use of an effective ionospheric height in electron content measurement by GPS reception. *Radio Sci.*, 37, 1, 1–19. DOI: 10.1029/2000RS002601
- Brunini, C., Camilion, E. and Azpilicueta, F.: 2011, Simulation study of the influence of the ionospheric layer height in the period-dependent layer ionospheric model. *J. Geod.*, 85, 9, 637–645. DOI: 10.1007/s00190-011-0470-2
- Komjathy, A., Sparks, L., Wilson, B.D. et al.: 2005, Automated daily processing of more than 1000 ground-based GPS receivers for studying intense ionospheric storms. *Radio Sci.*, 40, 6, 1–11. DOI: 10.1029/2005RS003279
- Lanyi, G.E. and Roth, T.: 1988, A comparison of mapped and measured total ionospheric electron content using global positioning system and beacon satellite observations. *Radio Sci.*, 23, 4, 483–492. DOI: 10.1029/RS023i004p00483
- Li, Z.: 2012, Study on the mitigation of ionospheric delay and the monitoring of global ionospheric TEC based on GNSS/Compass. Ph.D Thesis, Chinese Academy of Sciences, Beijing, (in Chinese).
- Li, Z., Wang, N., Wang, L. et al.: 2019, Regional ionospheric TEC modeling based on a two-layer spherical harmonic approximation for real-time single-frequency PPP. *J. Geod.*, 93, 9, 1659–1671. DOI: 10.1007/s00190-019-01275-5
- Li, M., Yuan, Y., Zhang, B. et al.: 2018, Determination of the optimized single-layer ionospheric height for electron content measurements over China. *J. Geod.*, 92, 2, 169–183. DOI: 10.1007/s00190-017-1054-6
- Mannucci, A.J., Iijima, B.A., Lindqwister, U.J. et al.: 1999, GPS and ionosphere. In: Stone, W.R., ed., *Review of Radio Science 1996–1999*, New York. Oxford University
- Nava, B., Radicella, S.M., Leitinger, R. et al.: 2007, Use of total electron content data to analyze ionosphere electron density gradients. *Adv. Space Res.*, 39, 8, 1292–1297. DOI: 10.1016/j.asr.2007.01.041
- Schaer, S.: 1999, Mapping and predicting the Earth's ionosphere using the global positioning system. Thesis, University of Berne, Berne, Sciences, Beijing, 228 pp. (in Chinese).
- Wang, N.: 2017, Study on GNSS differential code biases and global broadcast ionospheric models of GPS, Galileo and BDS. Ph.D Thesis, Institute Optoelectronics, Chinese Academy of Sciences, Beijing. DOI: 10.11947/j.AGCS.2017.20160387
- Wang, X.L., Wan, Q.T., Ma, G.Y. et al.: 2016, The influence of ionospheric thin shell height on TEC retrieval from GPS observation. *Res. Astron. Astrophys.*, 16, 7, 116–125. DOI: 10.1088/1674-4527/16/7/116
- Xu, L.: 2019, Study on BDS differential code biases estimation and the performance analysis of real-time ionospheric product. Thesis, China University of Mining and Technology, Xuzhou, (in Chinese).
- Xu, L., Chang, G., Gao J. et al.: 2021, Estimation of BDS DCB based on closure constraint. *Geomat. Inf. Sci. Wuhan Univ.*, 46, 4, 520–529. DOI: 10.13203/j.whugis.20190187
- Xu, L., Gao, J., Li, Z. et al.: 2020, Denoising ionospheric observables based on multipath error modelling with Tikhonov regularization. *Meas. Sci. Technol.*, 32, 2, 025801. DOI: 10.1088/1361-6501/abbc49
- Xu, L., Gao, J., Li, Z. et al.: 2023, A new flexible model to calibrate single-layer height for ionospheric modeling using a neural network model. *GPS Solut.*, 27, 3. DOI: 10.1007/s10291-023-01450-4
- Xu, L., Li, Z., Gao, J. et al.: 2022, Modelling short-term variations of differential code bias aiding in extraction of ionospheric observables with sparse kernel learning. *Adv. Space Res.*, 69, 7, 2836–2851. DOI: 10.1016/j.asr.2022.01.006
- Yuan, Y.: 2002, Study on theories and methods of correcting ionospheric delay and monitoring ionosphere based on GPS. Ph.D Thesis, Chinese Academy of Sciences, Wuhan. DOI: 10.13140/RG.2.2.14981.99041
- Yuan, Y., Huo, X. and Zhang, B.: 2017, Research progress of precise models and correction for GNSS ionospheric delay in China over recent years. *Acta Geod. Cartogr. Sin.*, 46, 10, 1364–1378, (in Chinese).
- Zhao, J. and Zhou, C.: 2018, On the optimal height of ionospheric shell for single-site TEC estimation. *GPS Solut.*, 2, 22, 1–11. DOI: 10.1007/s10291-018-0715-0